HDGF is not only highly expressed in a large number of different tumor types such as hepatocellular carcinoma (HCC), non-small cell lung cancer (NSCLC), and gastric adenocarcinoma, but it is also related to tumor invasion, metastasis and recurrence [10-17]. HDGF expression has been induced in the liver at a stage before HCC development, and it thereafter gradually increases during tumor growth in a rat hepatocarcinogenesis model [10]. Furthermore, HDGF has both an angiogenic activity as well as a cell growth stimulating activity [7, 18]. HDGF therefore appears to be a novel prognostic factor for patients suffering from different types of cancer [11-14, 16, 19-21]. HDGF is considered to be closely linked to carcinogenesis and the aggressive biological potential of tumor cells *in vivo*. However, the role of HDGF on HCC biology *in vivo* remains to be elucidated.

Previously we reported that HDGF over-expression in NIH3T3 induced a significant tumor formation in nude mice [7]. In the present study, HDGF over-expressing HepG2 cells were cloned and their biological functions for tumor growth were investigated by the use of an anchorage-independent colony formation assay in soft agar, xenograft tumor formation experiments and a DNA chip gene analysis.

MATERIALS AND METHODS

Anchorage-independent growth assay in soft agar

HDGF stably over-expressing HepG2 (HepG2-HDGF) and mock HepG2 (HepG2-neo) cells were established and maintained as reported previously [6]. The expression of myc-tagged HDGF and native HDGF was confirmed by Western blotting using polyclonal anti-C terminus of HDGF antibody at a dilution of 1 x 10,000.

To assess the anchorage independency of growth, 5,000 cells in 1.5 ml of 0.35% agar with DMEM were plated in each well on the top of an existing 0.5% bottom agar-DMEM in six-well tissue plates in triplicate for HepG2-HDGF and HepG2-neo, respectively. The cell colonies measuring > 0.1 mm in diameter were counted after 3 weeks of incubation at 37°C and 5% CO_2 in air, under a microscopic field at x 40 magnifications. The means were based on numbers from triplicate wells for each treatment condition and were analyzed using two-tailed Student's *t* test.

Tumorigenicity in nude mice

Four-week-old male BALB/cA Jcl-nu mice were obtained from Japan Clea (Hamamatsu, Japan). Following trypsinization, HeG2-HDGF and HepG2-Neo cells were harvested (2 x 10^6), resuspended in 200 µl of PBS and inoculated subcutaneously into left and right sides in the dorsal region of nude mouse. Two animals were used in each group. The tumor size was measured with a caliper once or twice per week, and the volumes were estimated according to the following formula: volume = maximal length x (perpendicular length)^2 x 0.5. A histological analysis of tumors which developed in the nude mice was performed after hematoxylin-eosin staining as reported previously [7].

DNA chip analysis

The total RNA was extracted from the cultured HepG2 cells and their xenograft tumor tissues using ISOGEN (Wako, Osaka, Japan) and Poly(A)+RNA was purified from total RNA using an Oligotex-Dt30 mRNA purification kit (Takara Otsu, Shiga, Japan).

The expression of each gene was simultaneously analyzed through the hybridization of the targets which were prepared by using Poly(A)+RNA as template. A DNA chip spotted with 886 cDNAs from identified human genes (IntelliGene™ Human CHIP 1K Set I, version 1.0) was acquired from Takara Shuzo, (Kyoto, Japan). The results were also analyzed by normalizing fluorescence intensities between experiments using a subset of cDNA clones.

Statistical analysis

The results are expressed as the means ± SE. At least three separate experiments were performed for each data point except for the DNA chip analysis. Statistical analyses were done using Student's unpaired *t*-test (two-tailed). Differences were considered to be statistically significant whenever a *P* value was < .05.

RESULTS

The over-expression of HDGF enhances the anchorage-independent growth of HCC cells in soft agar

We investigated whether the increased expression of HDGF stimulated the anchorage-independent growth of HCC cells in a soft agar assay. Three weeks after seeding, HepG2-HDGF cells produced significantly more and bigger colonies than HepG2-neo cells (Figure 1). The numbers of colonies (average of triplicate wells with three randomly selected fields per well) visible in a microscopic field at 40 magnifications for the two cell lines were 3.67±0.37 and 2.36±0.38 for HepG2-HDGF and HepG2-neo cells, respectively. These results suggest that HDGF enhances the anchorage-independent growth of HCC cells.

HDGF over-expression enhances the tumor growth of HCC cells *in vivo*

As shown in Figure 2, the HepG2-HDGF cells generated tumors at 4 weeks after injection, and these tumors increased in size over time. The tumor volume in the mice were 1,666±238 mm^3 and 442±26 mm^3 at 9 weeks after the inoculation of HepG2-HDGF and HepG2-neo cells, respectively ($P<0.01$). The tumors formed by HepG2-HDGF cells were macroscopically bigger and more reddish than those of HepG2-neo

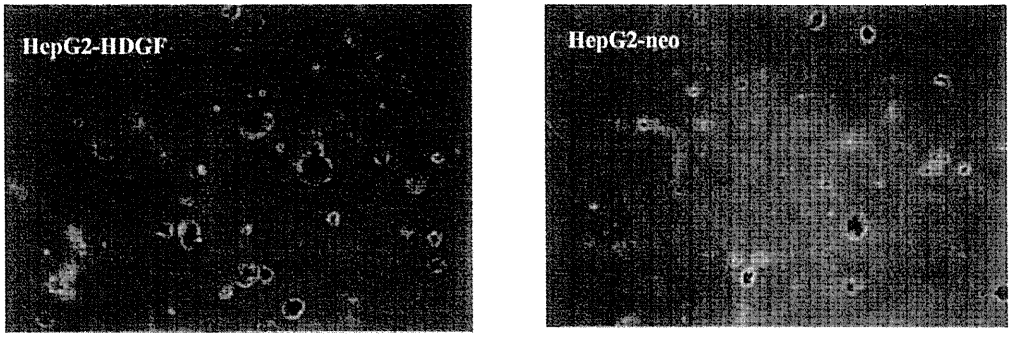

Figure 1. Effect of the HDGF over-expression on HCC cells in anchorage-independent growth. HDGF over-expressing HepG2 (HepG2-HDGF) cells produce larger colonies than mock HepG2 (HepG2-neo) cells in a soft agar assay described in Methods. The representative photos of colonies formed by HepG2-HDGF or HepG2-neo cells after 21-day culture were shown (x 40 magnifications).

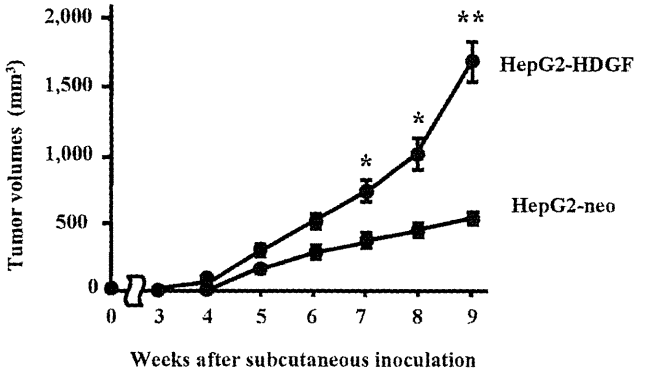

Figure 2. Tumor growth curves of HDGF over-expressing HepG2 cells in nude mice. The tumor volumes of HepG2-HDGF cells or HepG2-neo cells are shown after inoculation in nude mice. Data are shown as the mean ±SE of three independent experiments (n=3). *: $P<0.05$, and **: $P<0.01$, HepG2-HDGF vs. HepG2-neo.

cells (Figure 3a). Moreover, a microscopic examination showed abundant capillary vessel formation (Figure 3b). The expressions of the myc-tagged-HDGF protein in nude mice were confirmed by a Western blot analysis with rabbit polyclonal anti-C terminus of HDGF antibody (Figure 3c). These results suggest that an over-expression of HDGF stimulates the xenograft tumor growth rapidly in nude mice through prominent neovascularization as well as by stimulating the proliferation of cancer cells *in vivo*.

HDGF-regulated genes evaluated by a DNA chip analysis

We performed DNA chip analysis for both cultured cells and tumors generated in nude mice to investigate the up- and down-regulated genes by HDGF over-expression. DNA chip analysis revealed the genes which were differently expressed in HepG2-HDGF and HepG2-neo *in vitro* and *in vivo*. The top 10 genes up-regulated simultaneously both *in vitro* and *in vivo* by HDGF are shown in Table 1. Chitinase 3-like-2 and urokinase-type plasminogen activator (u-PA) were up-regulated more than 10 fold. Coagulation factor II receptor (F2R), matrix metalloproteinase 1 (MMP-1), platelet-derived growth factor alpha (PDGF-A), ankyrin 1, Ser-Thr protein kinase and A kinase anchor protein were up-regulated more than 2 fold. When we focus on the growth factors, growth factor-related proteins and their receptors, seven genes including PDGF-A were significantly up-regulated in the tumors generated from HepG2-HDGF cells in nude mice (Table 2). However, theses factors and receptors are induced more prominently *in vivo* than *in vitro* except for PDGF-A. Especially, Tyrosine kinase with Ig and EGF-like domains (Tie-1), schwannoma-derived growth factor (amphiregulin), AXL receptor tyrosine kinase are up-regulated more than 10 fold *in vivo*. On the other hand, the only gene that was down-regulated more than 2 fold by HDGF over-expression was connective tissue growth factor (CTGF), which decreased to 0.44 and 0.41 fold in cultured cells and xenograft tumors, respectively.

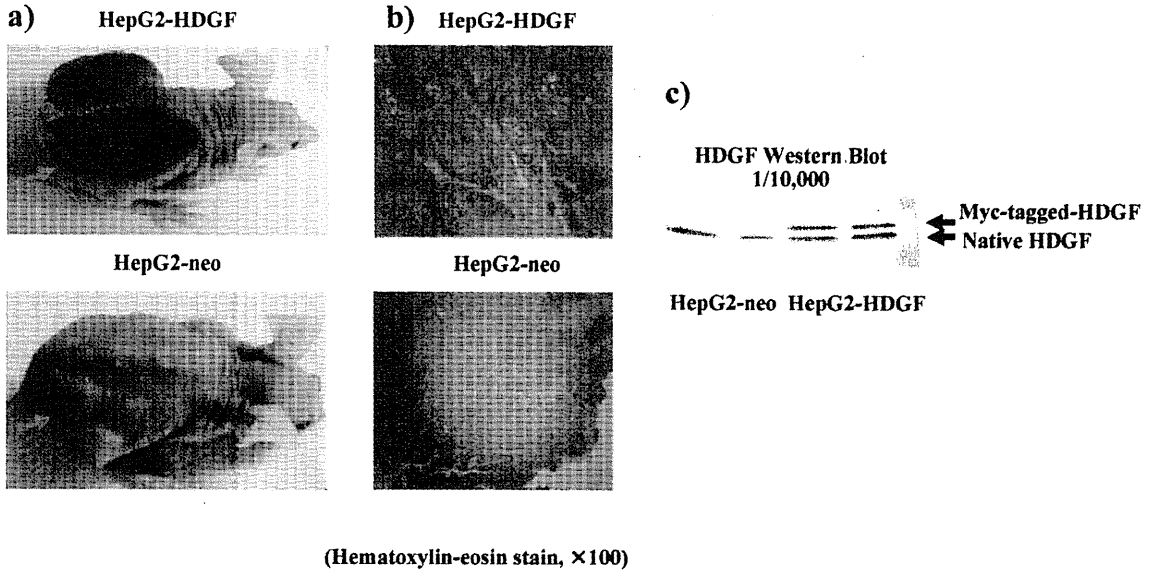

Figure 3. Tumors developed by the inoculation of HepG2-HDGF in nude mice.
a) The macroscopic appearance of tumors which developed in nude mice. Photographs show tumors that developed in the nude mice at 9 weeks after the subcutaneous inoculation of either HepG2-HDGF or HepG2-neo cells, respectively. b) Microscopic photographs of tumors which formed by HepG2-HDGF or HepG2-neo. Histological findings by hematoxylin-eosin staining show the tumors derived from HepG2-HDGF cells more rich in vasculature than HepG2-neo cells. c) The *in vivo* expression of myc-tagged-HDGF protein in each clone is shown in a Western blot analysis with rabbit polyclonal anti-C terminus HDGF antibody.

Table 1. The top 10 genes that were up-regulated in HepG2 cells by HDGF over-expression both *in vitro* and *in vivo*.

Genes	Rates of induction	
	Cell line	Nude mouse
Chitinase 3-like 2	17.99	9.42
Plasminogen activator, urokinase (u-PA)	17.97	4.77
Coagulation factor II receptor (F2R)	3.01	2.20
Matrix metalloproteinase 1 (MMP-1)	2.94	2.55
Platelet-derived growth factor alpha (PDGF-A)	2.59	3.85
Ankyrin 1	2.50	3.11
Ser-Thr protein kinase	2.30	3.51
A kinase (PPKA) anchor protein	2.24	2.06
Dystrophin	1.91	3.12
G protein-coupled receptor 105	1.89	3.51

Table 2. Top 7 genes of growth factors and their receptors that were up-regulated in tumors generated from HDGF over-expressing HepG2 cells in nude mice.

Genes	Rates of induction	
	Nude mouse	Cell line
Tyrosine kinase with Ig and EGF-like domains (Tie-1)	21.78	IC
Schwannoma-derived growth factor (Amphiregulin)	16.57	0.28
AXL receptor tyrosine kinase	14.05	IC
Bone morphogenetic protein 6 (BMP6)	6.43	IC
Leukemia inhibitory factor (LIF)	5.46	0.49
Epithelial cell receptor protein tyrosine kinase (EphA2)	4.82	0.31
Platelet-derived growth factor alpha polypeptide (PDGF-A)	3.85	2.59

IC: Incomparable due to no detectable signal in control or/and samples.

DISCUSSION

The established HepG2 clones which stably over-express HDGF stimulate not only the anchorage-independent colony formation in a soft agar, but also generate tumors and enhance the tumor growth in nude mice. Another study using gastric adenocarcinoma cells showed similar results, namely that HDGF transfection also promoted anchorage-independent growth in soft agar [17]. On the other hand, the down-regulated HDGF expression in non-small cell lung cancer (NSCLC) cells reduced the colony formation in soft agar and inhibited the invasive potential across the Matrigel membrane [9]. As reported previously, NIH3T3-HDGF cells generated tumors in nude mice, but the mock and wild NIH3T3 cells did not. The HDGF over-expression in NIH3T3 cells induced tumorigenesis *in vivo* through both a direct angiogenic activity and the induction of vascular endothelial growth factor (VEGF), but these HDGF-over-expressing cells could not form colonies of any significant size in soft agar [7]. NIH3T3 cells are a non-transformed cell line, derived from mouse fibroblasts. Conversely, HepG2 cell is a transformed cell line derived from hepatoblastoma cells as well as NSCLC cell line, A549 and gastric cancer cell

line, AGS [9, 17]. HDGF alone does not have the ability to form colonies of significant size in a soft agar assay, but it can generate tumors in nude mice. Therefore, other factor(s) are required to achieve *in vitro* anchorage-independent cell growth in soft agar, in addition to HDGF over-expression. In cancer derived transformed cells, these factors have already been expressed and then HDGF produced a large number of colonies of significant size of cancer cells in soft agar. *In vivo*, both HDGF over-expressing NIH3T3 cells and HepG2 cells generated tumors in nude mice. Therefore, HDGF may be responsible for both tumor formation and growth *in vivo*.

Down-regulated HDGF in NSCLC cells inhibits the tumor growth and markedly reduces blood vessel formation in nude mice [9]. In the present study, HDGF over-expression was observed to promote tumor growth, while also stimulating vessel formation in nude mice. HDGF can directly stimulate the endothelial cell proliferation and induce VEGF, thus resulting in prominent angiogenesis *in vivo* [7]. According to the DNA chip results both *in vitro* and *in vivo*, another vascular growth factor, PDGF-A is up-regulated by an over-expression of HDGF. PDGF-A is a growth factor which is closely related to the proliferation of HCC cells [22]. Therefore, these findings suggest that HDGF promotes the tumor growth *in vivo* through the enhanced angiogenesis by the induction of these angiogenic factors in addition to its direct angiogenic activity.

Some genes related to the biologically aggressive characteristics of tumors including invasion and metastasis are up-regulated by HDGF over-expression both *in vitro* and *in vivo* according to a DNA chip analysis. The up-regulation of chitinase 3-like-2 is associated with a poor survival in glioblastoma, and an over-expression of ankyrin has been reported to contribute to hepatocarcinogenesis by destabilizing the retinoblastoma gene [23, 24]. The down regulation of u-PA by small interfering RNA has been reported to suppress the invasion and migration of human HCC cells [25]. Another up-regulated gene, MMP-1 is also closely involved in tumor invasion. MMP-1 is expressed in early HCC, and conversely the reduced activity of MMP-1 by MMP inhibitor potently suppresses the invasion of HCC cells [26, 27]. Therefore, HDGF may display either an invasive or metastatic activity through the induction of these genes.

Furthermore, when we focus on these growth factors, their receptors and signal transduction proteins, some molecules related in tumor biology are up-regulated by an HDGF over-expression in tumors which developed *in vivo*. The Tie-1 expression is up-regulated at 22 fold in tumors derived from HepG2-HDGF cells in comparison to those from HepG2-neo cells *in vivo*, but it is not up-regulated in cells *in vitro*. Tie-1, which is predominantly expressed in blood vessel endothelial cells, is deeply involved in angiogenesis [28]. Tie-1 is reported to be highly expressed in large HCCs and may be a novel independent prognostic marker for gastric cancer [29, 30]. Tie-1 may be involved in the rich vasculature in HepG2-HDGF-derived tumors, after its induction in endothelial cells by the paracrine effect of HDGF. AXL is up-regulated by 14 fold in tumors from HepG2-HDGF cells in comparison to those from HepG2-neo cells. AXL has been reported to be highly expressed in multiple types of cancers including HCC, and it has also been linked to an adverse clinical outcome in patients with cancer [31]. Interestingly, AXL has been demonstrated to be significantly down-regulated by HDGF siRNA treatment in NSCLC-derived tumors in nude mice [9]. These facts suggest that AXL induction by HDGF may thus play an important role as one pathway to display the biological aggressiveness of cancers.

Conversely, only one gene, CTGF is down-regulated by HDGF over-expression in HepG2 cells and their xenograft tumors. CTGF exhibits a variety of biological functions of tumor cells, including cell adhesion, migration and proliferation. An elevated expression of CTGF has been detected in several cancers, and the inhibition of CTGF with a monoclonal antibody suppresses pancreatic tumor growth and metastasis [32]. An increased expression of CTGF was associated with a decreased survival of patients with breast cancer, glioblastoma or esophageal adenocarcinoma [33-35]. In contrast, a high level of CTGF has been reported to be associated with better survival in patients with

esophageal squamous cell carcinoma and chondrosarcoma, and its reduced expression has also been shown to be correlated with the disease stage and decreased survival in lung adenocarcinoma [35-37]. In HCC, CTGF has been reported to be highly expressed, however the relationship between the CTGF levels and the disease-free or overall survivals in patients with HCC has not yet been clarified [38, 39]. The down-regulation of CTGF by HDGF suggests that the reduced expression of CTGF may be related to an advanced disease stage and the malignant potentials in HCC cells. Further studies should thus be conducted to elucidate the role of CTGF on HCC cells.

In conclusion, we confirmed that HDGF over-expression in HCC cell lines promoted the anchorage-independent growth of HCC cells and the xenograft tumor formation, and regulated the expression of the genes which were related to tumor biology. These findings are consistent with the clinical evidence that a higher expression of HDGF in tumors has more aggressive characteristics, including distant metastasis and invasion, and a higher recurrence and poorer survival. Therefore, HDGF promotes tumorigenesis and tumor progression not only through its direct angiogenic activity and cell proliferation stimulating activity but also due to the up-regulation and down-regulation of the genes, that are involved in tumor biology and angiogenesis. Future studies should focus on analyzing the detailed molecular mechanisms of HDGF-induced tumor development and progression, in order to eventually develop a treatment modality to regulate the action of HDGF protein and the molecules related in its signal transduction pathway in order to develop potential therapeutically effective applications.

ABBREVIATIONS

HDGF, hepatoma-derived growth factor; PDGF, platelet-derived growth factor; CTGF, connective tissue growth factor; Tie-1, tyrosine kinase with Ig and EGF-like domains; u-PA, urokinase-type plasminogen activator; MMP-1, matrix metallo-proteinase 1; HCC, hepatocellular carcinoma; NSCLC, non-small cell lung cancer

REFERENCES

1. Nakamura, H., Kambe, H., Egawa, T., Kimura, Y., Ito, H., Hayashi, E., Yamamoto, H., Sato, J., and Kishimoto, S. 1989, Clin. Chim. Acta, 183, 273.
2. Nakamura, H., Izumoto, Y., Kambe, H., Kuroda, T., Mori, T., Kawamura, K., Yamamoto, H., and Kishimoto, T. 1994, J. Biol. Chem., 269, 25143.
3. Oliver, J, A., and Al-Awqati, Q. 1998, J. Clin. Invest., 102, 1208.
4. Everett, A. D., Lobe, D. R., Matsumura, M. E., Nakamura, H., and McNamara, C. A. 2000, J. Clin. Invest., 105, 567.
5. Everett, A. D., Stoops, T., and McNamara, C. A. 2001, J. Biol. Chem., 276, 37564.
6. Kishima, Y., Yamamoto, H., Izumoto, Y., Yoshida, K., Enomoto, H., Yamamoto, M., Kuroda, T., Ito, H., Yoshizaki, K., Nakamura, H. 2002, J. Biol. Chem., 277, 10315.
7. Okuda, Y., Nakamura, H., Yoshida, K., Enomoto, H., Uyama, H., Hirotani, T., Funamoto, M., Ito, H., Everett, A. D., Hada, T., and Kawase, I. 2003, Cancer Sci., 94, 1034.
8. Kishima, Y., Yoshida, K., Enomoto, H., Yamamoto, M., Kuroda, T., Okuda, Y., Uyama, H., and Nakamura, H. 2002, Hepatogastroenterology, 49, 1639.
9. Zhang, J., Ren, H., Yuan, P., Lang, W., Zhang, L., and Mao, L. 2006, Cancer Res., 66, 18.
10. Yoshida, K., Nakamura, H., Okuda, Y., Enomoto, H., Kishima, Y., Uyama, H., Ito, H., Hirasawa, T., Inagaki, S., and Kawase, I. 2003, J. Gastroenterol. Hepatol., 18, 1293.
11. Hu, T. H., Huang, C. C., Liu, L. F., Lin, P. R., Liu, S. Y., Chang, H. W., Changchien, C. S., Lee, C. M., Chuang, J. H., and Tai, M. H. 2003, Cancer, 98, 1444.
12. Yoshida, K., Tomita, Y., Okuda, Y., Yamamoto, S., Enomoto, H., Uyama, H., Ito, H., Hoshida, Y., Aozasa, K., Nagano, H., Sakon, M., Kawase, I., Monden, M., and Nakamura, H. 2006, Ann. Surg. Oncol., 13, 1.
13. Ren, H., Tang, X., Lee, J. J., Feng, L., Everett, A. D., Hong, W. K., Khuri, F. R., and Mao, L. 2004, J. Clin. Oncol., 22, 3230.

14. Iwasaki, T., Nakagawa, K., Nakamura, H., Takada, Y., Matsui, K., and Kawahara, K. 2005, Oncol. Rep., 13, 1075.
15. El-Rifai, W., Frierson, H. F. Jr., Harper, J. C., Powell, S. M., and Knuutila, S. 2001, Int. J. Cancer., 92, 832.
16. Yamamoto, S., Tomita, Y., Hoshida, Y., Takiguchi, S., Fujiwara, Y., Yasuda, T., Doki, Y., Yoshida, K., Aozasa, K., Nakamura, H., and Monden, M. 2006, Clin. Cancer Res., 12, 117.
17. Mao, J., Xu, Z., Fang, Y., Wang, H., Xu, J., Ye, J., Zheng, S., and Zhu, Y. 2008, Cancer Sci., 99, 2120.
18. Everett, A. D., Narron, J. V., Stoops, T., Nakamura, H., and Tucker, A. 2004, Am. J. Physiol. Lung Cell Mol. Physiol., 286, L1194.
19. Yamamoto, S., Tomita, Y., Hoshida, Y., Morii, E., Yasuda, T., Doki, Y., Aozasa, K., Uyama, H., Nakamura, H., and Monden, M. 2007, Ann. Surg. Oncol., 14, 2141.
20. Uyama, H., Tomita, Y., Nakamura, H., Nakamori, S., Zhang, B., Hoshida, Y., Enomoto, H., Okuda, Y., Sakon, M., Aozasa, K., Kawase, I., Hayashi, N., and Monden, M. 2006, Clin. Cancer Res., 12 (20 Pt 1), 6043.
21. Chang, K. C., Tai, M. H., Lin, J. W., Wang, C. C., Huang, C. C., Hung, C. H., Chen, C. H., Lu, S. N., Lee, C. M., Changchien, C. S., and Hu, T. H. 2007, Int. J. Cancer, 121, 1059.
22. Stock, P., Monga, D., Tan, X., Micsenyi, A., Loizos, N., and Monga, S. P. 2007, Mol. Cancer Ther., 6, 1932.
23. Saidi, A., Javerzat, S., Bellahcène, A., De Vos, J., Bello, L., Castronovo, V., Deprez, M., Loiseau, H., Bikfalvi, A., and Hagedorn, M. 2008, Int. J. Cancer, 122, 2187.
24. Higashitsuji, H., Itoh, K., Nagao, T., Dawson, S., Nonoguchi, K., Kido, T., Mayer, R. J., Arii, S., and Fujita, J. 2000, Nat. Med., 6, 96.
25. Salvi, A., Arici, B., De Petro, G., and Barlati, S. 2004, Mol. Cancer Ther., 3, 671.
26. Murakami, K., Sakukawa, R., Ikeda, T., Matsuura, T., Hasumura, S., Nagamori, S., Yamada, Y., and Saiki, I. 1999, Neoplasia., 1, 424.
27. Okazaki, I., Wada, N., Nakano, M., Saito, A., Takasaki, K., Doi, M., Kameyama, K., Otani, Y., Kubochi, K., Niioka, M., Watanabe, T., and Maruyama, K. 1997, Hepatology, 25, 580.
28. Tang, Y., Borgstrom, P., Maynard, J., Koziol, J., Hu, Z., Garen, A., and Deisseroth, A. 2007, Cancer Gene Ther., 14, 346.
29. Dhar, D. K., Naora, H., Yamanoi, A., Ono, T., Kohno, H., Otani, H., and Nagasue, N. 2002, Anticancer Res., 22(1A), 379.
30. Lin, W. C., Li, A. F., Chi, C. W., Chung, W. W., Huang, C. L., Lui, W. Y., Kung, H. J., and Wu, C. W. 1999, Clin. Cancer Res., 5, 1745.
31. Tsou, A. P., Wu, K. M., Tsen, T. Y., Chi, C. W., Chiu, J. H., Lui, W. Y., Hu, C. P., Chang, C., Chou, C. K., and Tsai, S. F. 1998, Genomics, 50, 331.
32. Dornhöfer, N., Spong, S., Bennewith, K., Salim, A., Klaus, S., Kambham, N., Wong, C., Kaper, F., Sutphin, P., Nacamuli, R., Höckel, M., Le, Q., Longaker, M., Yang, G., Koong, A., and Giaccia, A. 2006, Cancer Res., 66, 5816.
33. Xie, D., Nakachi, K., Wang, H., Elashoff, R., and Koeffler, H. P. 2001, Cancer Res., 61, 8917.
34. Xie, D., Yin, D., Wang, H. J., Liu, G. T., Elashoff, R., Black, K., and Koeffler, H. P. 2004, Clin. Cancer Res., 10, 2072.
35. Koliopanos, A., Friess, H., di Mola, F. F., Tang, W. H., Kubulus, D., Brigstock, D., Zimmermann, A., and Büchler, M. W. 2002, World J. Surg., 26, 420.
36. Shakunaga, T., Ozaki, T., Ohara, N., Asaumi, K., Doi, T., Nishida, K., Kawai, A., Nakanishi, T., Takigawa, M., and Inoue, H. 2000, Cancer, 89, 1466.
37. Chang, C. C., Shih, J. Y., Jeng, Y. M., Su, J. L., Lin, B. Z., Chen, S. T., Chau, Y. P., Yang, P. C., and Kuo, M. L. 2004, J. Natl. Cancer Inst., 96, 364.
38. Hirasaki, S., Koide, N., Ujike, K., Shinji, T., and Tsuji, T. 2001, Hepatol. Res., 19, 294.
39. Zeng, Z. J., Yang, L. Y., Ding, X., and Wang, W. 2004, World J. Gastroenterol., 10, 3414.

DOI:10.1158/1535-7163.MCT-10-0544

Preclinical Development

Molecular Cancer Therapeutics

Sorafenib Inhibits the Hepatocyte Growth Factor–Mediated Epithelial Mesenchymal Transition in Hepatocellular Carcinoma

Tomoyuki Nagai[1,2], Tokuzo Arao[1], Kazuyuki Furuta[1], Kazuko Sakai[1], Kanae Kudo[1,2], Hiroyasu Kaneda[1], Daisuke Tamura[1], Keiichi Aomatsu[1], Hideharu Kimura[1], Yoshihiko Fujita[1], Kazuko Matsumoto[1], Nagahiro Saijo[3], Masatoshi Kudo[2], and Kazuto Nishio[1]

Abstract

The epithelial mesenchymal transition (EMT) has emerged as a pivotal event in the development of the invasive and metastatic potentials of cancer progression. Sorafenib, a VEGFR inhibitor with activity against RAF kinase, is active against hepatocellular carcinoma (HCC); however, the possible involvement of sorafenib in the EMT remains unclear. Here, we examined the effect of sorafenib on the EMT. Hepatocyte growth factor (HGF) induced EMT-like morphologic changes and the upregulation of SNAI1 and N-cadherin expression. The downregulation of E-cadherin expression in HepG2 and Huh7 HCC cell lines shows that HGF mediates the EMT in HCC. The knockdown of SNAI1 using siRNA canceled the HGF-mediated morphologic changes and cadherin switching, indicating that SNAI1 is required for the HGF-mediated EMT in HCC. Interestingly, sorafenib and the MEK inhibitor U0126 markedly inhibited the HGF-induced morphologic changes, SNAI1 upregulation, and cadherin switching, whereas the PI3 kinase inhibitor wortmannin did not. Collectively, these findings indicate that sorafenib downregulates SNAI1 expression by inhibiting mitogen-activated protein kinase (MAPK) signaling, thereby inhibiting the EMT in HCC cells. In fact, a wound healing and migration assay revealed that sorafenib completely canceled the HGF-mediated cellular migration in HCC cells. In conclusion, we found that sorafenib exerts a potent inhibitory activity against the EMT by inhibiting MAPK signaling and SNAI1 expression in HCC. Our findings may provide a novel insight into the anti-EMT effect of tyrosine kinase inhibitors in cancer cells. *Mol Cancer Ther; 10(1); 169–77. ©2011 AACR.*

Introduction

Hepatocellular carcinoma (HCC) is the fifth most common cancer and the third largest cause of cancer-related death in the world annually (1). Recurrence, metastasis, and the development of new primary tumors are the most common causes of mortality among patients with HCC (2). Sorafenib (Nexavar; Bayer HealthCare Pharmaceuticals Inc.) is a small molecule that inhibits the kinase activities of Raf-1 and B-Raf in addition to VEGFRs, PDGFR-β (platelet-derived growth factor receptor β), Flt-3, and c-KIT (3). Two recent randomized controlled trials reported a clinical benefit of single-agent sorafenib in extending overall survival in both Western and Asian patients with advanced unresectable HCC (4, 5). The potential action mechanisms that lead to these clinical benefits are thought to include antiangiogenic effects and sorafenib's characteristic inhibitory effect on Raf-1 and B-Raf signaling.

Meanwhile, growing evidence indicates that the epithelial mesenchymal transition (EMT), a developmental process by which epithelial cells reduce intercellular adhesions and acquire fibroblastoid properties, has important roles in the development of the invasive and metastatic potentials of cancer progression (6–8). To date, numerous clinicopathologic studies have shown positive correlations between the expressions of the transcription factors SNAI1 (snail homologue 1/SNAIL) and SNAI2 (snail homologue 2/Slug), which are key inducible factors of the EMT, and poor clinical outcomes in breast, ovary, colorectal, and lung cancer; squamous cell carcinoma; melanoma, and HCC (reviewed in ref. 6).

Generally, the activation of a wide variety of ligands including FGF (fibroblast growth factor), TGF-β–BMPs (bone morphogenetic protein), Wnt, EGF (epidermal growth factor), VEGF, and HGF (hepatocyte growth factor) and its receptor can upregulate the expression of EMT-regulating transcription factors, including SNAI1, SNAI2, ZEB1, ZEB2, and TWIST (6). Among them, HGF (also known as scattering factor) activates

Authors' Affiliations: Departments of [1]Genome Biology, [2]Gastroenterology and [3]Medical Oncology, Kinki University School of Medicine, Japan

Note: Supplementary material for this article is available at Molecular Cancer Therapeutics Online (http://mct.aacrjournals.org/).

Corresponding Author: Kazuto Nishio, Department of Genome Biology, Kinki University School of Medicine, 377-2 Ohno-higashi, Osaka-Sayama, Osaka 589-8511, Japan. Phone: 81-72-366-0221 (ext 3150); Fax: 81-72-367-6369; E-mail: knishio@med.kindai.ac.jp

doi: 10.1158/1535-7163.MCT-10-0544

DOI:10.1158/1535-7163.MCT-10-0544

the Met signaling pathway, thereby increasing the invasive and metastatic potentials of the cells and allowing the survival of cancer cells in the bloodstream in the absence of anchorage (9). In addition, HGF is well known as a potent angiogenic cytokine, and Met signal activation can modify the microenvironment to facilitate cancer progression (9). Therefore, the HGF-Met signaling pathway is regarded as a promising therapeutic target, and many molecular targeted drugs are under clinical development (10). In HCC, the mRNA levels of HGF and Met receptor are markedly increased compared with those in normal liver (11). A high serum HGF concentration is associated with a poor prognosis for overall survival after hepatic resection, and the serum level of HGF represents the degree of the carcinogenic state in the livers of patients with C-viral chronic hepatitis and cirrhosis (12–14). Thus, we examined the effect of sorafenib on the HGF-Met–mediated EMT in HCC.

Materials and Methods

Reagents

Sorafenib was provided by Bayer HealthCare Pharmaceuticals Inc. U0126, wortmannin (Cell Signaling Technology), and human HGF (R&D Systems) were purchased from the indicated companies. The structures of compounds are shown in Supplementary Figure 1.

Cell culture

The human HCC cell lines HepG2 and Huh7 were maintained in Dulbecco's modified Eagle's (DMEM) medium (Sigma) supplemented with 10% FBS, penicillin, and streptomycin (Sigma) in a humidified atmosphere of 5% CO_2 at 37°C. The cell lines were obtained from the Japanese Collection of Research Bioresources and were grown in culture for less than 6 months.

Scratch assay

The method used for the scratches assay has been previously described (15). Briefly, the cells were plated onto 24-well plates and incubated in DMEM containing 10% FBS until they reached subconfluence. Scratches were introduced to the subconfluent cell monolayer, using a plastic pipette tip. The cells were then cultured with DMEM containing 10% FBS at 37°C. After 24 hours, the scratch area was photographed using a light microscope (IX71; Olympus). The wound distance between edge to edge were measured and averaged from 5 points per 1 wound area, using DP manager software (Olympus). The 2 wound areas were evaluated in an experiment and the experiment was done in triplicate.

Migration assay

The migration assays were done using the Boyden chamber methods and polycarbonate membranes with an 8-μm pore size (Chemotaxicell), as previously described (15). The membranes were coated with fibronectin on the outer side and dried for 2 hours at room temperature. The cells to be analyzed (2×10^4 cells/well) were then seeded onto the upper chambers with 200 μL of migrating medium (DMEM containing 0.5% FBS), and the upper chambers were placed into the lower chambers of 24-well culture dishes containing 600 μL of DMEM containing 10% FBS or with 10 ng/mL of HGF or with HGF and 10 μmol/L of sorafenib. After incubation for 36 hours (HepG2) and 24 hours (Huh7), the media in the upper chambers were aspirated and the nonmigrated cells on the inner sides of the membranes were removed using a cotton swab. The cells that had migrated to the outer side of the membranes were fixed with 4% paraformaldehyde for 10 minutes, stained with 0.1% Giemsa stain solution for 15 minutes, and then counted using a light microscope. Migrated cells were averaged from 5 fields per 1 chamber and 3 chambers were used on 1 experiment. The experiment was done in triplicate.

Morphologic analysis

HepG2 and Huh7 cells (2×10^4 and 1×10^4 cells/well, respectively) were seeded in 6-well tissue culture dishes. After 24 hours of incubation, the cells were stimulated with 10 ng/mL of HGF or control PBS. When the inhibitors were used, the cells were exposed to each inhibitor for 3 hours before the addition of HGF. After 48 hours, the cells were analyzed using a light microscope. The experiment was done in triplicate.

Western blot analysis

The following antibodies were used in this study: phospho-Met (Y1349), Met, phospho-AKT (S473), AKT, phospho-p44/42 mitogen-activated protein kinase (MAPK), SNAI1/Snail, E-cadherin, N-cadherin, vimentin, β-actin antibody horseradish peroxidase–conjugated secondary antibody (Cell Signaling Technology), and fibronectin (Santa Cruz Biotechnology). All the experiments were done at least in duplicate. The Western blot analysis was done as described previously (16). The data were quantified by automated densitometry using Multigauge Ver. 3.0 (Fujifilm). Densitometric data were normalized by β-actin in triplicate and the average was shown above the Western blot as a ratio of control sample.

Real-time reverse transcription PCR

The real-time reverse transcription PCR (RT-PCR) method has been previously described (17). Briefly, 1 μg of total RNA from the cultured cells was converted to cDNA using a GeneAmp RNA-PCR kit (Applied Biosystems). Real-time RT-PCR amplification was done using a Thermal Cycler Dice (Takara) in accordance with the manufacturer's instructions under the following conditions: 95°C for 6 minutes, 40 cycles of 95°C for 15 seconds, and 60°C for 1 minute. Glyceraldehyde 3-phosphate dehydrogenase (GAPD) was used to normalize the expression levels in the subsequent quantitative analyses. To amplify the target genes, the following primers were purchased from TaKaRa: *CDH1*, forward 5′-TTA AAC

DOI:10.1158/1535-7163.MCT-10-0544

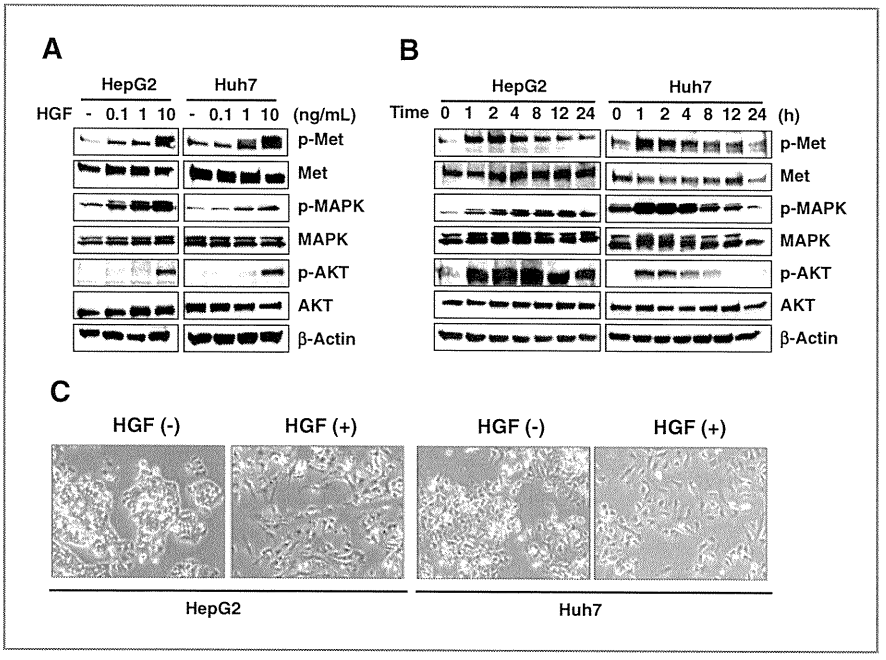

Figure 1. HGF stimulates the Met signaling pathway and induces morphologic changes in HCC. A, HGF stimulation (0, 0.1, 1, and 10 ng/mL) dose-dependently increased the phosphorylation of Met, MAPK, and AKT in the HCC cell lines HepG2 and Huh7. The results of a Western blot analysis are shown. β-Actin was used as a loading control. The serum-starved cells were stimulated with HGF for 60 minutes and then collected for analysis. B, time-course analysis of HGF stimulation. The HCC cells were stimulated with 10 ng/mL of HGF for 0, 1, 2, 4, 8, 12, and 24 hours. The results of a Western blot analysis are shown. C, HGF-mediated morphologic changes included cell scattering and the elongation of the cell shape that are characteristic of the EMT. The HepG2 and Huh7 cells were stimulated with or without 10 ng/mL of HGF for 48 hours and then photographed (magnification × 200).

TCC TGG CCT CAA GCA ATC-3′ and reverse 5′-TCC TAT CTT GGG CAA AGC AAC TG-3′; *CDH2*, forward 5′-CGA ATG GAT GAA AGA CCC ATC C-3′ and reverse 5′-GGA GCC ACT GCC TTC ATA GTC AA-3′; *SNAI1*, forward 5′-TCT AGG CCC TGG CTG CTA CAA-3′ and reverse 5′-ACA TCT GAG TGG GTC TGG AGG TG-3′; *SNAI2*, forward 5′-ATG CAT ATT CGG ACC CAC ACA TTA C-3′ and reverse 5′-AGA TTT GAC CTG TCT GCA AAT GCT C-3′; *VIM*, forward 5′-TGA GTA CCG GAG ACA GGT GCA G-3′ and reverse 5′-TAG CAG CTT CAA CGG CAA AGT TC-3′; *FN1*, forward 5′-GGA GCA AAT GGC ACC GAG ATA-3′ and reverse 5′-GAG CTG CAC ATG TCT TGG GAA C-3′; and *GAPD*, forward 5′-GCA CCG TCA AGG CTG AGA AC-3′ and reverse 5′-ATG GTG GTG AAG ACG CCA GT-3′.

Small interfering RNA transfection

Three different sequences of small interfering RNA (siRNA) targeting human SNAI1 (Hs_SNAI1_9785, 9786, and 9787) and those of 2 scramble control siRNAs were purchased from Sigma Aldrich Japan. The transfection methods have been previously described (17).

Statistical analysis

The statistical analyses were done using Microsoft Excel (Microsoft) both to calculate the SD and to test for statistically significant differences between the samples using a Student t test. A value $P < 0.05$ was considered statistically significant.

Results

To examine the activity of HGF-Met signaling in HCC cells, we examined the expressions of phospho-Met, Met, phospho-AKT, AKT, phospho-MAPK, and MAPK in the HepG2 and Huh7 cell lines, using Western blotting. The phosphorylation levels of Met, AKT, and MAPK were dose-dependently increased by HGF stimulation (Fig. 1A). A time-course analysis showed that the phosphorylation levels of Met, AKT, and MAPK peaked at 1 to 2 hours after HGF stimulation and gradually recovered to the baseline values at 4 hours later (Fig. 1B). These results indicated that Met signaling is actually capable of being activated in response to HGF in HCC cells.

From a morphologic aspect, the EMT is characterized by an increase in cell scattering and an elongation of the cell shape (18). To evaluate whether HGF mediates the morphologic change that is characteristic of the EMT in HCC cells, cellular morphology was examined after HGF stimulation. HGF clearly mediated both cell scattering and the elongation of the cell shape in HepG2 and Huh7 cell lines (Fig. 1C). These data indicate that HGF mediates

DOI:10.1158/1535-7163.MCT-10-0544

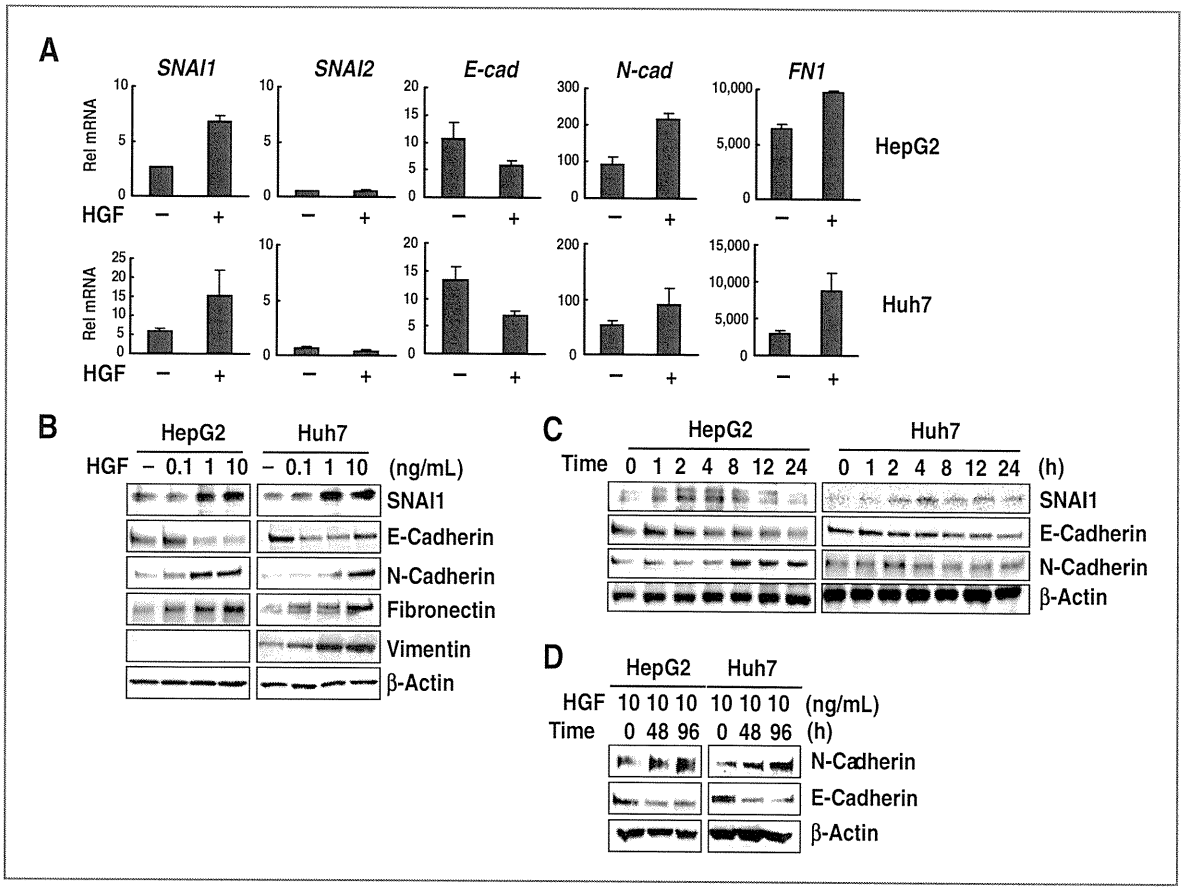

Figure 2. HGF upregulates SNAI1 expression and induces cadherin switching in HCC. A, changes in the mRNA expressions of the EMT-related genes *SNAI1/Snail*, *SNAI2/Slug*, *E-cadherin/CDH1*, *N-cadherin/CDH2*, and *fibronectin/FN1* were determined using real-time RT-PCR. The HepG2 and Huh7 cells were stimulated with or without 10 ng/mL of HGF for 2 hours (SNAI1 and SNAI2) or 48 hours (*E-cad*, *N-cad*, and *FN1*). Rel mRNA, normalized mRNA expression levels (target genes/GAPD $\times 10^4$); E-cad, E-cadherin; N-cad, N-cadherin. B, the HGF-mediated protein expression changes in SNAI1, E-cadherin, N-cadherin, fibronectin, and vimentin were determined using a Western blot analysis. The HepG2 and Huh7 cells were stimulated with HGF at the indicated dose (0, 0.1, 1, or 10 ng/mL) and collected for analysis after 4-hour stimulation for SNAI1 and 72 hours for the others. C, the cells were stimulated with 10 ng/mL of HGF for the indicated time course (0, 1, 2, 4, 8, 12, or 24 hours) and used for analysis. β-Actin was used as a loading control. D, Western blot analysis of E-cadherin and N-cadherin. The cells were stimulated with 10 ng/mL of HGF for 0, 48, and 96 hours and then analyzed.

the morphologic changes that are compatible with the induction of the EMT in HCC cell lines.

Because SNAI1 and SNAI2 are considered to be master regulators of the EMT, changes in the mRNA expression levels of EMT-related genes in response to HGF stimulation were evaluated using real-time RT-PCR (Fig. 2A). HGF stimulation upregulated SNAI1 mRNA expression by more than 2-fold, whereas the baseline expression of SNAI2 was very low compared with that of SNAI1 and did not respond to HGF in either of the HCC cell lines that were examined. Cadherin switching, which is characterized by the downregulation of E-cadherin and the upregulation of N-cadherin, is known as one of the most pivotal cellular events in the EMT (19). Cadherin switching was clearly observed on the basis of mRNA levels after HGF stimulation. The mesenchymal marker fibronectin was also upregulated (Fig. 2A).

Consistent with the mRNA changes, HGF stimulation dose-dependently upregulated the protein expression of SNAI1, N-cadherin, fibronectin, and vimentin and downregulated the expression of E-cadherin in both cell lines (Fig. 2B). Vimentin expression of HepG2 was not detected (baseline vimentin mRNA was also extremely low; data not shown). A time-course analysis showed that HGF upregulated the SNAI1 expression at 2 hours after stimulation and that the expression level recovered to the baseline value at 24 hours thereafter (Fig. 2C). Cadherin switching after HGF stimulation was observed at 8 hours later in HepG2 cells and 48 hours later in Huh7 cells (Fig. 2C and D). Generally, upregulation of SNAI1 is

DOI:10.1158/1535-7163.MCT-10-0544

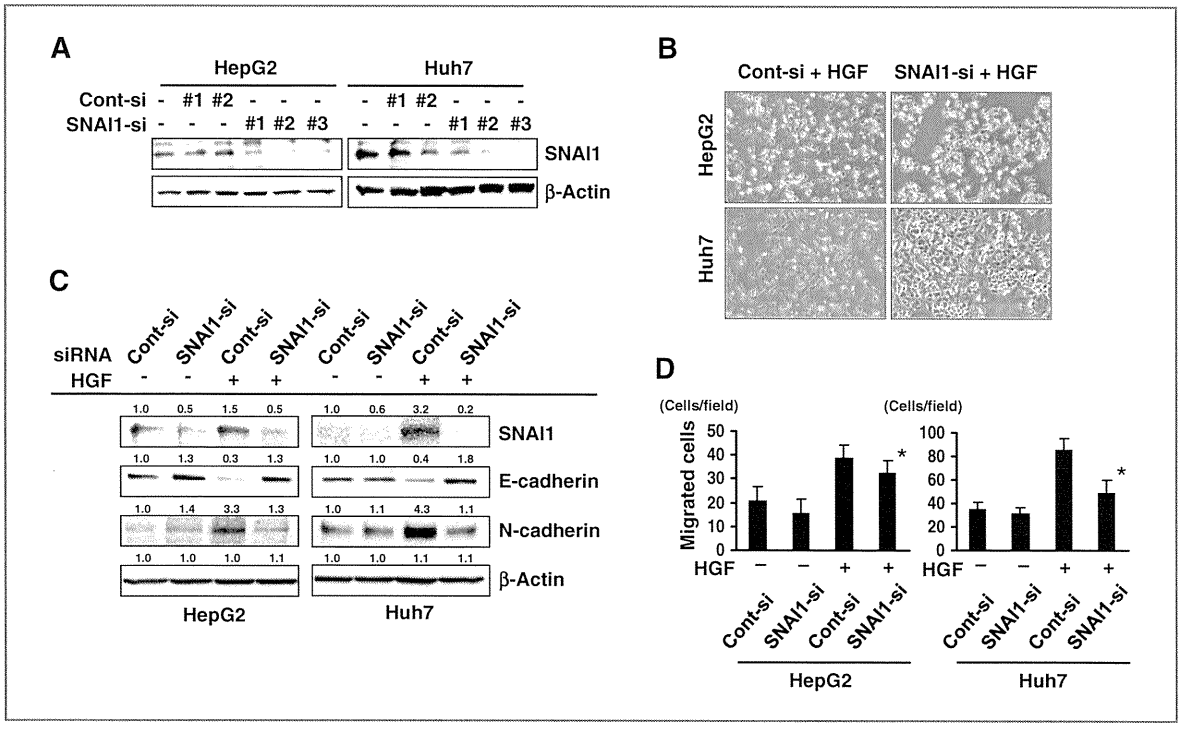

Figure 3. SNAI1 is required to induce the HGF-mediated EMT in HCC cells. A, knockdown of HGF-mediated SNAI1 expression using siRNA. Three sequences of SNAI1-siRNA (1, 2, and 3) were used. The HepG2 and Huh7 cells were treated with or without 50 nmol/L of each siRNA for 48 hours and then were stimulated with 10 ng/mL of HGF. SNAI1-siRNA #2 was effective and was used in subsequent experiments. B, SNAI1 knockdown canceled the HGF-mediated morphologic changes. The HepG2 and Huh7 cells were treated with 50 nmol/L of siRNA for 48 hours and were then stimulated with 10 ng/mL of HGF in all 4 panels. C, SNAI1 suppression by siRNA strongly canceled the HGF-mediated downregulation of E-cadherin and the upregulation of N-cadherin in both HepG2 and Huh7 cells. The cells were treated with 50 nmol/L of siRNA for 48 hours and were analyzed using a Western blot analysis. Densitometric data are shown above the Western blot. D, the siRNA knockdown of SNAI1 inhibited the HGF-mediated cellular migration. The siRNA-transfected HepG2 and Huh7 cells were evaluated using migration assay. The migration assays were conducted using the Boyden chamber methods as described in Materials and Methods. *, $P < 0.05$ (Cont-si vs. SNAI1-si with HGF); Cont-si, control-siRNA; SNAI1-si, SNAI1-targeting siRNA.

observed within few hours, but cadherin switching occurs around 24 hours later after stimulation (20, 21), consistent with our result. These results indicate that HGF meditates the induction of SNAI1, cadherin switching, and the EMT in HCC cells.

Besides SNAI1 and SNAI2, other transcription factors of several genes also have the potential to repress E-cadherin and to induce the EMT; these factors include ZEB1/TCF8, ZEB2/SMAD interacting protein 1, TWIST, E47/TCF3, and TCF4/E2-2 (6). Therefore, we examined whether SNAI1, among several EMT-inducible genes, has a central role in the HGF-mediated EMT in HCC cells. Three sequences of SNAI1-siRNA (1, 2, and 3) were used. A Western blot showed that both sequences 2 and 3 of SNAI1-siRNA completely suppressed the HGF-mediated upregulation of SNAI1 in the HepG2 and Huh7 cells (Fig. 3A); thus, the #2 SNAI1-siRNA was used in the following experiments: The siRNA knockdown of SNAI1 canceled the morphologic changes observed in HepG2 cells undergoing HGF-mediated EMT, whereas the control-siRNA did not (Fig. 3B). Similar results were obtained in Huh7 cells, indicating that SNAI1 is required for the morphologic changes observed in HGF-mediated EMT. Similarly, the siRNA knockdown of SNAI1 strongly canceled the HGF-mediated downregulation of E-cadherin and the upregulation of N-cadherin in both HepG2 and Huh7 cells (Fig. 3C). Those of mRNA expression changes were relatively correlated with the results of Western blot, except for N-cadherin in Huh7 cells (Supplementary Fig. 2A). Regarding the cellular migration, the siRNA knockdown of SNAI1 inhibited the HGF-mediated cellular migration (Fig. 3D). Collectively, these results indicate that SNAI1 is required to induce the HGF-mediated EMT in HCC cells.

In general, SNAI1 expression is regulated by ligand-receptor signal transduction through a downstream signal pathway that includes the Smad, MAPK, AKT, and GSK3 pathways (6, 22, 23). Sorafenib has been shown to inhibit RAF-MAPK signaling in HCC cells (24). Accordingly, we hypothesized that sorafenib might downregulate SNAI1 expression by inhibiting RAF-MAPK signaling, which is a unique activity of sorafenib. As

DOI:10.1158/1535-7163.MCT-10-0544

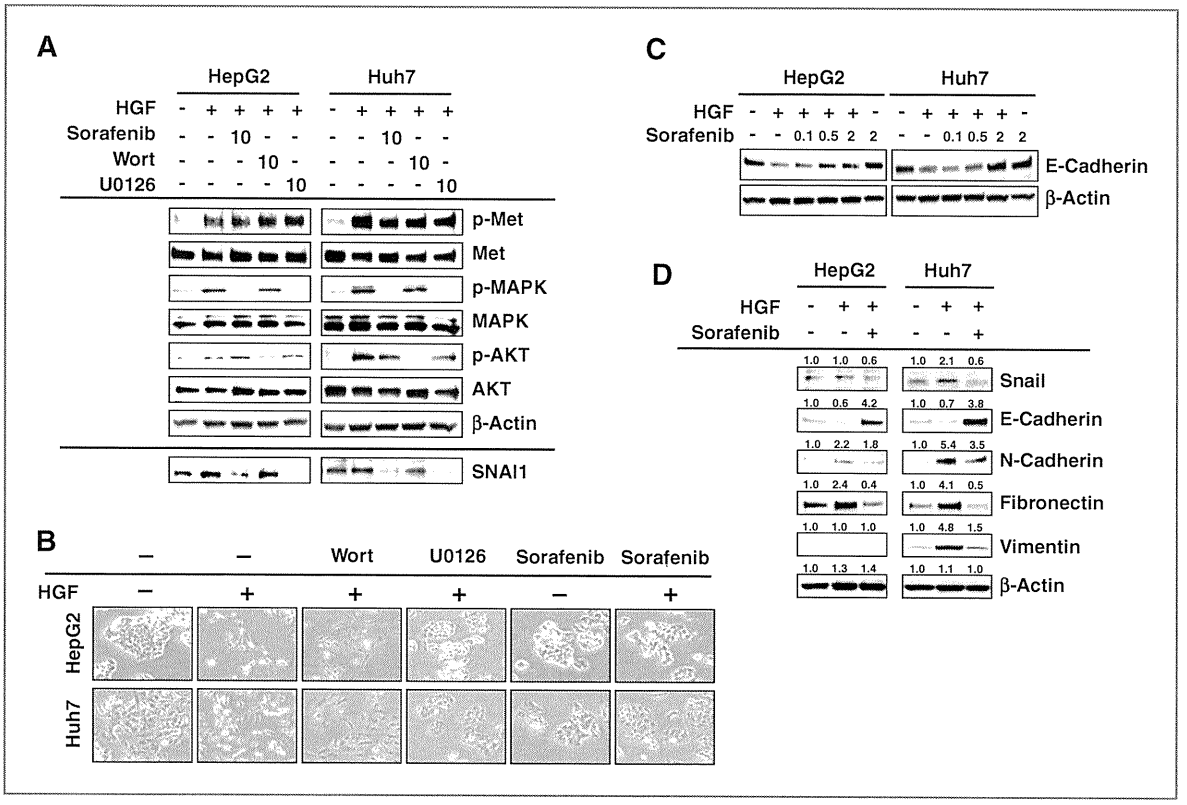

Figure 4. Sorafenib downregulates SNAI1 expression in HCC. A, as expected, sorafenib and the MEK inhibitor U0126 inhibited the HGF-mediated phosphorylation of MAPK, but the PI3K inhibitor wortmannin did not. Of note, SNAI1 expression was markedly downregulated by sorafenib and U0126. The HepG2 and Huh7 cells were exposed to 10 μmol/L of sorafenib or wortmannin or U0126 for 3 hours and were then stimulated with 10 ng/mL of HGF for 60 minutes. Wort, wortmannin. B, the HGF-mediated morphologic changes were canceled by sorafenib and U0126 but not by wortmannin in the HCC cells. The cells were exposed to sorafenib or wortmannin or U0126 for 48 hours with or without HGF (10 ng/mL) and then photographed. C, HGF-mediated downregulation of E-cadherin was canceled by sorafenib. The cells were stimulated with HGF (10 ng/mL) and treated with sorafenib at indicated concentration for 48 hours. D, HGF-mediated cadherin switching and upregulation of fibronectin and vimentin were canceled by sorafenib in the HCC cell lines. The cells were cultured with or without 2 μmol/L of sorafenib for 72 hours, with or without HGF (10 ng/mL), and then were analyzed using Western blot analysis. Densitometric data are shown above the Western blot.

expected, sorafenib and the MEK inhibitor U0126 (10 μmol/L) markedly inhibited the HGF-induced phosphorylation of MAPK, but the PI3K inhibitor wortmannin (10 μmol/L) did not. In contrast, only wortmannin inhibited the phosphorylation of AKT (Fig. 4A). Notably, SNAI1 expression was strongly downregulated by sorafenib and U0126 but not by wortmannin (Fig. 4A). These results showed that sorafenib downregulated SNAI1 expression via MAPK signaling. Meanwhile, we examined the HGF- and sorafenib-mediated expression changes of *SNAI2*, *ZEB1*, *ZEB2*, and *TWIST* using real-time RT-PCR and Western blot (Supplementary Fig. 3). Baseline and expression changes of SNAI2 and TWIST were very low compared with SNAI1, and the expression changes of ZEB1 and ZEB2 seemed not to be significant. Collectively, we considered that SNAI2, TWIST, ZEB1, and ZEB2 are not likely to be involved in the effect of HGF and sorafenib on EMT in this cell lines. Then, we examined the activity of sorafenib on HGF-mediated morphologic changes in HCC cells. HGF stimulation mediated the cell scattering and spindle-shaped changes, and these effects were clearly canceled by sorafenib and U0126, but not by wortmannin, in both HepG2 and Huh7 cells (Fig. 4B). These results were consistent with the results of Western blotting. To show whether sorafenib cancels the effect of HGF-mediated downregulation of E-cadherin, we examined the Western blot in dose–response analysis. Downregulation of E-cadherin was clearly canceled by sorafenib in a dose-dependent manner (Fig. 4C). Time-course analysis showed that HGF-mediated downregulation of E-cadherin was also canceled by sorafenib (Supplementary Fig. 4). HGF stimulation downregulated E-cadherin expression and upregulated N-cadherin, vimentin, and fibronectin in HCC cells; however, these effects were canceled by sorafenib in both HCC cell lines (Fig. 4D and Supplementary Fig. 2B). The mRNA data of N-cadherin in Huh7 cells were not correlated with protein level. These results show that sorafenib inhibits the

DOI:10.1158/1535-7163.MCT-10-0544

RAF-MAPK pathway, thereby downregulating SNAI1 and inhibiting the EMT in HCC.

Because sorafenib inhibits the HGF-mediated EMT in HCC cells, we next examined whether the inhibitory effect of sorafenib on the EMT leads to an inhibition of cellular migration in HCC cells. A scratch assay revealed that HGF stimulation increased cellular migration by about 2- fold in both HCC cell lines; however, sorafenib significantly inhibited this effect to the baseline levels (Fig. 5A). Similarly, a migration assay using the Boyden chamber method revealed that sorafenib canceled HGF-mediated cellular migration in both cell lines (Fig. 5B). These results suggest that sorafenib actually inhibits the cellular migrating phenotype of the EMT in HCC cells. The combination of migration data with siRNA and sorafenib (Fig. 3D and Fig. 5B) suggests that inhibitory effects of sorafenib on migration may be mediated by Snail downregulation in some tumors (e.g., Huh7) but not in others (e.g., HepG2). It is assumed that the inhibitory activity of sorafenib on the cellular migrating phenotype is due to its inhibitory effect of Raf-MAPK signaling pathway (Fig. 4A and B). Regarding HGF-dependent PI3K-AKT signaling pathway, wortmannin weakly inhibited the wound closure in Huh7 cells and to the same extent by sorafenib in HepG2 cells (Supplementary Fig. 5). In contrast, wortmannin has no effect on Snail levels or on HCC morphology changes (Fig. 4A and B). Collectively, we speculate that activation of HGF-dependent PI3K-AKT pathway may not be involved in SNAI1 induction or morphologic change but at least partially involved in cell migration independent of Raf-MAPK-SNAI1 signaling.

Taken together, these results indicate that sorafenib inhibits the HGF-mediated EMT, which is characterized by cadherin switching, morphologic changes, and an increase in the cellular migrating phenotype, by inhibiting Raf-MAPK signaling, resulting in the downregulation of SNAI1 in HCC cells (Fig. 6).

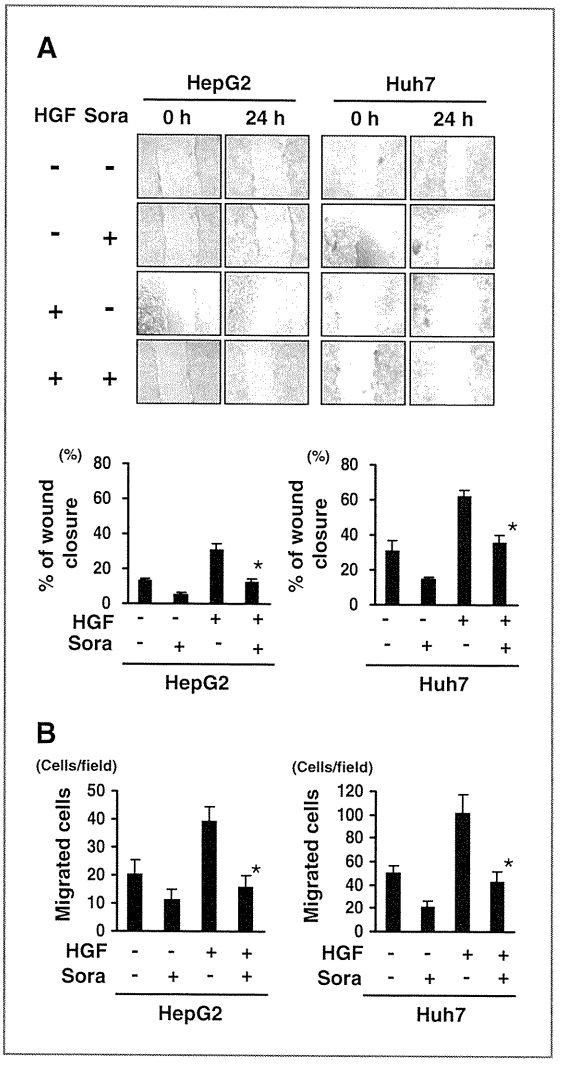

Figure 5. Sorafenib inhibits HGF-mediated cellular migration in HCC cells. A, a scratch assay revealed that HGF stimulation increased the cellular migration by about 2-fold, but sorafenib almost completely canceled the effect. The subconfluent HepG2 and Huh7 cells were scratched with a plastic pipette tip and incubated under the indicated conditions (control, 10 ng/mL of HGF; and HGF, 10 μmol/L of sorafenib). The scratch area was photographed and measured. The experiment was done in triplicate. *, sorafenib (−) versus (+), $P < 0.05$. B, migration assay using the Boyden chamber method revealed that sorafenib almost completely canceled the HGF-mediated cellular migration in both HCC cell lines. The cells were incubated under the indicated conditions: control, 10 ng/mL of HGF; and HGF, 10 μmol/L of sorafenib. *, sorafenib (−) versus (+), $P < 0.05$. Sora, sorafenib.

Discussion

Recent accumulating evidence has shown that the EMT is involved in drug sensitivity to several anticancer agents (25). Within this topic, the most intensively investigated drugs have been endothelial growth factor receptor (EGFR)–targeting drugs for the treatment of lung cancer. A clinical trial has revealed that lung cancer cells with strong E-cadherin expression exhibit a significantly longer time to progression after EGFR-TKI (tyrosine kinase inhibitor) treatment (26). Other studies on EGFR-targeting drugs have shown that mesenchymal type lung cancer cells exhibit an EMT-dependent acquisition of PDGFR, FGF receptor, and TGF-β receptor signaling pathways (27), and integrin-linked kinase is a novel target for overcoming HCC resistance to EGFR inhibition (28). Regarding sensitivity to gemcitabine, mesenchymal type cancer cells are reportedly associated with gemcitabine resistance in pancreatic cancer cells (29). The mechanism of resistance to gemcitabine has been shown to involve the activation of Notch signaling, which is mechanistically linked with the mesenchymal chemoresistance phenotype of pancreatic cancer cells (30). Thus, baseline cellular characteristics based on the EMT phenotype might be useful not only as prognostic biomarkers for a malignant phenotype but also as predictive markers

DOI:10.1158/1535-7163.MCT-10-0544

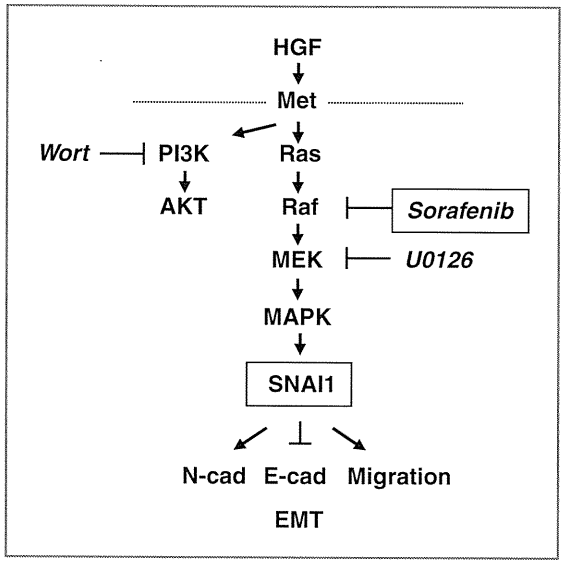

Figure 6. Diagram of the proposed mechanism by which sorafenib inhibits the EMT. Sorafenib inhibits the HGF-mediated EMT, which is characterized by morphologic changes, cadherin switching, and an increase in the cellular migrating phenotype. The anti-EMT effect of sorafenib occurs through the downregulation of SNAI1 by the inhibition of MAPK phosphorylation in HCC cells. Wort, wortmannin; N-cad, N-cadherin; E-cad, E-cadherin.

of sensitivity to anticancer agents. In this study, we focused on the signaling pathway responsible for inducing the EMT and showed that the multitarget TKI sorafenib downregulates SNAI1 by inhibiting Raf-MAPK signaling, thereby inhibiting the HGF-mediated EMT in HCC cells. Our findings may provide a novel insight into the actions of TKIs and their anti-EMT effects.

The mechanisms underlying the SNAI1-induced metastatic and aggressive phenotypes of cancer cells have recently been intensively investigated in both basic and clinical research studies. A novel aspect of the activity of SNAI1 is its involvement in immunosuppression. The SNAI1-induced EMT mediates regulatory T cells and impairs dendritic cells, accelerating cancer metastasis not only by enhancing invasion but also by inducing immunosuppression (31). A complex of histone deacetylase (HDAC) and SNAI1 plays an essential role in silencing E-cadherin (32), suggesting that the use of HDAC inhibitors to inhibit SNAI1 function might represent a promising therapeutic approach. On the other hand, large-scale clinical data on SNAI1 expression and the prognosis of patients with HCC were recently reported (33) and the overexpression of SNAI2 and/or TWIST was correlated with a worse prognosis. In contrast, no such significant differences were observed in samples that overexpressed SNAI2. The coexpression of Snail and TWIST was correlated with the worst prognosis for HCC (33). This evidence suggests that SNAI1 might be a useful therapeutic target for oncology. Our findings showed that sorafenib completely canceled the HGF-mediated SNAI1 induction in HepG2 and Huh7 cells. This activity of sorafenib, in addition to sorafenib's anti-angiogenic effects, might contribute to a clinical benefit against metastatic and aggressive phenotypes in patients with HCC.

Disclosure of Potential Conflicts of Interest

No potential conflicts of interest were disclosed.

Acknowledgments

We thank Tomoko Kitayama and the staff of the Life Science Research Institute for their technical assistance.

Grant Support

This work was supported in part by the Third-Term Comprehensive 10-Year Strategy for Cancer Control and a Grant-in-Aid for Cancer Research (H20-20-9) from the Ministry of Health and Labor Scientific Research Grants.

The costs of publication of this article were defrayed in part by the payment of page charges. This article must therefore be hereby marked *advertisement* in accordance with 18 U.S.C. Section 1734 solely to indicate this fact.

Received June 9, 2010; revised October 25, 2010; accepted October 25, 2010; published online January 10, 2011

References

1. Jemal A, Murray T, Ward E, et al. Cancer statistics, 2005. CA Cancer J Clin 2005;55:10–30.
2. Yamamoto J, Kosuge T, Takayama T, et al. Recurrence of hepatocellular carcinoma after surgery. Br J Surg 1996;83:1219–22.
3. Wilhelm SM, Carter C, Tang L, et al. BAY 43-9006 exhibits broad spectrum oral antitumor activity and targets the RAF/MEK/ERK pathway and receptor tyrosine kinases involved in tumor progression and angiogenesis. Cancer Res 2004;64:7099–109.
4. Llovet JM, Ricci S, Mazzaferro V, et al.; SHARP Investigators Study Group. Sorafenib in advanced hepatocellular carcinoma. N Engl J Med 2008;359:378–90.
5. Cheng AL, Kang YK, Chen Z,, et al. Efficacy and safety of sorafenib in patients in the Asia-Pacific region with advanced hepatocellular carcinoma: a phase III randomised, double-blind, placebo-controlled trial. Lancet Oncol 2009;10:25–34.
6. Peinado H, Olmeda D, Cano A. Snail, Zeb and bHLH factors in tumour progression: an alliance against the epithelial phenotype?Nat Rev Cancer 2007;7:415–28.
7. Hugo H, Ackland ML, Blick T, et al. Epithelial-mesenchymal and mesenchymal-epithelial transitions in carcinoma progression. J Cell Physiol 2007;213:374–83.
8. Tsuji T, Ibaragi S, Hu GF. Epithelial-mesenchymal transition and cell cooperativity in metastasis. Cancer Res 2009;69:7135–9.
9. Gentile A, Trusolino L, Comoglio PM. The Met tyrosine kinase receptor in development and cancer. Cancer Metastasis Rev 2008;27:85–94.
10. Eder JP, Vande Woude GF, Boerner SA, LoRusso PM. Novel therapeutic inhibitors of the c-Met signaling pathway in cancer. Clin Cancer Res 2009;15:2207–14.
11. Yang H, Magilnick N, Noureddin M, Mato JM, Lu SC. Effect of hepatocyte growth factor on methionine adenosyltransferase genes

DOI:10.1158/1535-7163.MCT-10-0544

and growth is cell density-dependent in HepG2 cells. J Cell Physiol 2007;210:766–73.
12. Mizuguchi T, Nagayama M, Meguro M, et al. Prognostic impact of surgical complications and preoperative serum hepatocyte growth factor in hepatocellular carcinoma patients after initial hepatectomy. J Gastrointest Surg 2009;13:325–33.
13. Chau GY, Lui WY, Chi CW, et al. Significance of serum hepatocyte growth factor levels in patients with hepatocellular carcinoma undergoing hepatic resection. Eur J Surg Oncol 2008;34:333–8.
14. Yamagamim H, Moriyama M, Matsumura H, et al. Serum concentrations of human hepatocyte growth factor is a useful indicator for predicting the occurrence of hepatocellular carcinomas in C-viral chronic liver diseases. Cancer 2002;95:824–34.
15. Tanaka K, Arao T, Maegawa M, et al. SRPX2 is overexpressed in gastric cancer and promotes cellular migration and adhesion. Int J Cancer 2009;124:1072–80.
16. Matsumoto K, Arao T, Tanaka K, et al. mTOR signal and hypoxia-inducible factor-1 alpha regulate CD133 expression in cancer cells. Cancer Res 2009;69:7160–4.
17. Kaneda H, Arao T, Tanaka K, et al. FOXQ1 is overexpressed in colorectal cancer and enhances tumorigenicity and tumor growth. Cancer Res 2010;70:2053–63.
18. Lee JM, Dedhar S, Kalluri R, Thompson EW: The epithelial-mesenchymal transition: new insights in signaling, development, and disease. J Cell Biol 2006;172:973–81.
19. Wheelock MJ, Shintani Y, Maeda M, Fukumoto Y, Johnson KR. Cadherin switching. J Cell Sci 2008;121:727–35.
20. Lo HW, Hsu SC, Xia W, et al. Epidermal growth factor receptor cooperates with signal transducer and activator of transcription 3 to induce epithelial-mesenchymal transition in cancer cells via up-regulation of TWIST gene expression. Cancer Res 2007;67:9066–76.
21. Vincent T, Neve EP, Johnson JR, et al. A SNAIL1-SMAD3/4 transcriptional repressor complex promotes TGF-beta mediated epithelial-mesenchymal transition. Nat Cell Biol 2009;11:943–50.
22. Larue L, Bellacosa A. Epithelial-mesenchymal transition in development and cancer: role of phosphatidylinositol 3' kinase/AKT pathways. Oncogene 2005;24:7443–54.
23. Zavadil J, Böttinger EP. TGF-beta and epithelial-to-mesenchymal transitions. Oncogene 2005;24:5764–74.
24. Liu L, Cao Y, Chen C, et al. Sorafenib blocks the RAF/MEK/ERK pathway, inhibits tumor angiogenesis, and induces tumor cell apoptosis in hepatocellular carcinoma model PLC/PRF/5. Cancer Res 2006;66:11851–8.
25. Voulgari A, Pintzas A. Epithelial-mesenchymal transition in cancer metastasis: mechanisms, markers and strategies to overcome drug resistance in the clinic. Biochim Biophys Acta 2009;1796:75–90.
26. Yauch RL, Januario T, Eberhard DA, et al. Epithelial versus mesenchymal phenotype determines *in vitro* sensitivity and predicts clinical activity of erlotinib in lung cancer patients. Clin Cancer Res 2005; 11:8686–98.
27. Thomson S, Petti F, Sujka-Kwok I, Epstein D, Haley JD. Kinase switching in mesenchymal-like non-small cell lung cancer lines contributes to EGFR inhibitor resistance through pathway redundancy. Clin Exp Metastasis 2008;25:843–54.
28. Fuchs BC, Fujii T, Dorfman JD, et al. Epithelial-to-mesenchymal transition and integrin-linked kinase mediate sensitivity to epidermal growth factor receptor inhibition in human hepatoma cells. Cancer Res 2008;68:2391–9.
29. Arumugam T, Ramachandran V, Fournier KF, et al. Epithelial to mesenchymal transition contributes to drug resistance in pancreatic cancer. Cancer Res 2009;69:5820–8.
30. Wang Z, Li Y, Kong D, et al. Acquisition of epithelial-mesenchymal transition phenotype of gemcitabine-resistant pancreatic cancer cells is linked with activation of the notch signaling pathway. Cancer Res 2009;69:2400–7.
31. Kudo-Saito C, Shirako H, Takeuchi T, Kawakami Y. Cancer metastasis is accelerated through immunosuppression during Snail-induced EMT of cancer cells. Cancer Cell 2009;15:195–206.
32. von Burstin J, Eser S, Paul MC, et al. E-cadherin regulates metastasis of pancreatic cancer *in vivo* and is suppressed by a SNAIL/HDAC1/HDAC2 repressor complex. Gastroenterology 2009;137:361–71.
33. Yang MH, Chen CL, Chau GY, et al. Comprehensive analysis of the independent effect of Twist and Snail in promoting metastasis of hepatocellular carcinoma. Hepatology 2009;50:1464–74.

Published OnlineFirst December 3, 2010; DOI:10.1158/1078-0432.CCR-09-2755

Cancer Therapy: Preclinical

Clinical Cancer Research

Antitumor Activity of BIBF 1120, a Triple Angiokinase Inhibitor, and Use of VEGFR2$^+$pTyr$^+$ Peripheral Blood Leukocytes as a Pharmacodynamic Biomarker *In Vivo*

Kanae Kudo[1,2], Tokuzo Arao[1], Kaoru Tanaka[1], Tomoyuki Nagai[1], Kazuyuki Furuta[1], Kazuko Sakai[1], Hiroyasu Kaneda[1], Kazuko Matsumoto[1], Daisuke Tamura[1], Keiichi Aomatsu[1], Marco A. De Velasco[1], Yoshihiko Fujita[1], Nagahiro Saijo[3], Masatoshi Kudo[2], and Kazuto Nishio[1]

Abstract

Purpose: BIBF 1120 is a potent, orally available triple angiokinase inhibitor that inhibits VEGF receptors (VEGFR) 1, 2, and 3, fibroblast growth factor receptors, and platelet-derived growth factor receptors. This study examined the antitumor effects of BIBF 1120 on hepatocellular carcinoma (HCC) and attempted to identify a pharmacodynamic biomarker for use in early clinical trials.

Experimental Design: We evaluated the antitumor and antiangiogenic effects of BIBF 1120 against HCC cell line both *in vitro* and *in vivo*. For the pharmacodynamic study, the phosphorylation levels of VEGFR2 in VEGF-stimulated peripheral blood leukocytes (PBL) were evaluated in mice inoculated with HCC cells and treated with BIBF 1120.

Results: BIBF 1120 (0.01 μmol/L) clearly inhibited the VEGFR2 signaling *in vitro*. The direct growth inhibitory effects of BIBF 1120 on four HCC cell lines were relatively mild *in vitro* (IC_{50} values: 2–5 μmol/L); however, the oral administration of BIBF 1120 (50 or 100 mg/kg/d) significantly inhibited the tumor growth and angiogenesis in a HepG2 xenograft model. A flow cytometric analysis revealed that BIBF 1120 significantly decreased the phosphotyrosine (pTyr) levels of VEGFR2$^+$CD45^{dim} PBLs and the percentage of VEGFR2$^+$pTyr$^+$ PBLs *in vivo*; the latter parameter seemed to be a more feasible pharmacodynamic biomarker.

Conclusions: We found that BIBF 1120 exhibited potent antitumor and antiangiogenic activity against HCC and identified VEGFR2$^+$pTyr$^+$ PBLs as a feasible and noninvasive pharmacodynamic biomarker *in vivo*. *Clin Cancer Res; 17(6); 1373–81. ©2010 AACR.*

Introduction

A number of antiangiogenic inhibitors have been studied in clinical settings, some of which have clearly exhibited a clinical benefit in oncology. Consequently, VEGFs and VEGF receptors (VEGFR) are now well-validated targets in cancer therapy (1). In hepatocellular carcinoma (HCC), 2 recent randomized controlled trials for HCC have reported a clinical benefit of single-agent sorafenib for extending the overall survival in both Western and Asian patients with advanced unresectable HCC (2, 3). On the basis of the clear results of these trials, sorafenib is presently regarded as the standard therapy for HCC.

Because antiangiogenic inhibitors may achieve therapeutic levels long before toxicities arise compared with conventional cytotoxic chemotherapies, identifying pharmacodynamic biomarkers that accurately reflect the effects of the drug on its known targets are needed (4, 5). Therefore, a wide variety of biomarkers of antiangiogenic inhibitors have been proposed and intensively investigated, including plasma proteins, angiogenesis-related signaling, immunohistochemistry of endothelial cell markers for evaluating microvessel density (MVD), circulating endothelial progenitor/cells, and functional imaging such as dynamic contrast-enhanced MRI and molecular imaging using positron emission tomography (6). These candidate biomarkers have been evaluated and characterized as prognostic, pharmacodynamic, or response-predictive markers. Although the utility of biomarkers for evaluating MVD was highly anticipated, these markers were not predictive for clinical response in patients treated with bevacizumab (7). Regarding growth factors and cytokines, the plasma VEGF level has been shown to be neither a pharmacodynamic nor a predictive biomarker of antiangiogenic drugs (7, 8), although the plasma VEGF level is a well-known prognostic biomarker (9–11). Plasma-soluble VEGFR2, on the other hand, may be a promising and specific biomarker of

Authors' Affiliations: Departments of [1]Genome Biology and [2]Gastroenterology, [3]Kinki University School of Medicine, Osaka, Japan

Note: Supplementary data for this article are available at Clinical Cancer Research Online (http://clincancerres.aacrjournals.org/).

Corresponding Author: Kazuto Nishio, Department of Genome Biology, Kinki University School of Medicine, 377-2 Ohno-higashi, Osaka-Sayama, Osaka 589-8511, Japan. Phone: 81-72-366-0221; Fax: 81-72-366-0206. E-mail: knishio@med.kindai.ac.jp

doi: 10.1158/1078-0432.CCR-09-2755

Published OnlineFirst December 3, 2010; DOI:10.1158/1078-0432.CCR-09-2755

Translational Relevance

A wide variety of biomarkers of antiangiogenic inhibitors have been proposed and intensively investigated; however, no biomarkers have been validated for routine clinical use and a new pharmacodynamic biomarker is needed. We have shown in this study that (i) BIBF 1120, a VEGF receptor 2 (VEGFR2) inhibitor, exhibited potent antitumor and antiangiogenic activity against hepatocellular carcinoma *in vivo* and (ii) $VEGFR2^{+}pTyr^{+}$ peripheral blood leukocytes (PBL) were useful pharmacodynamic biomarker *in vivo*. Our findings indicate the clinical utility of $VEGFR2^{+}pTyr^{+}$ PBLs as a feasible, noninvasive, and VEGF signal-specific biomarker of VEGFR2 tyrosine kinase inhibitors for use in early clinical trials.

antiangiogenic drugs for evaluating their effects (12, 13). Indeed, we have shown that soluble VEGFR2 was certainly decreased by BIBF 1120 treatment in a phase I trial; however, this decrease was observed at a relatively late stage, 8 to 29 days after the start of treatment (14). These results suggest that soluble VEGFR2 is not a rapid-responding biomarker for monitoring effects of antiangiogenic drugs. As no other biomarkers have been validated for routine clinical use, a new pharmacodynamic biomarker is needed.

BIBF 1120 is a potent triple angiokinase inhibitor that inhibits VEGFR1, 2, and 3, fibroblast growth factor receptors (FGFR), and platelet-derived growth factor receptors (PDGFR). *In vitro* studies have shown that VEGFR2 tyrosine kinase activity was potently inhibited by BIBF 1120 (IC_{50} = 21 nmol/L) and was also active against VEGFR1 and 3 (IC_{50} = 34 and 13 nmol/L, respectively; ref. 15). BIBF 1120 dose dependently inhibited the growth of various human tumor xenografts and tumor angiogenesis *in vivo* studies, consistent with the potent inhibition of VEGF signaling (15). BIBF 1120 also exhibited a relatively strong direct growth inhibitory effect on cancer cell lines, influencing 9 of 14 acute myeloid leukemia cell lines in a colony formation assay with an IC_{50} value of less than 1 μmol/L (16).

We previously reported the antitumor activity of VEGFR2 tyrosine kinase inhibitors (TKI) against non–small cell lung cancer and gastric cancer, identifying a biomarker and the mode of action (17–19). In the present study, we focused on the antitumor activity of BIBF 1120 against HCC, which is hypervascular in nature. In addition, to identify a pharmacodynamic biomarker, we examined the phosphorylation levels of VEGFR-positive peripheral blood leukocytes (PBL) as a surrogate tissue in an *in vivo* model.

Materials and Methods

Compounds

BIBF 1120 was provided by Boehringer Ingelheim Pharma GmbH & KG. 5-Fluorouracil (5FU; Sigma-Aldrich) and an epidermal growth factor receptor (EGFR) TKI, AG1478 (Biomol International), were purchased from the indicated companies.

Cell lines and cultures

HepG2, HLF, HLE, and Huh7 (human hepatoblastoma and HCC cell lines, respectively) were maintained in Dulbecco's modified Eagle's medium supplemented with 10% FBS (Gibco BRL). HUVECs (human umbilical vein endothelial cells) were purchased from Kurabo and were maintained in Humedia-EG2 (Kurabo) medium with 2% FBS, 2 ng/mL of VEGF-A (R&D Systems), 10 ng/mL of EGF, 5 ng/mL of FGF, 10 μg/mL of heparin, and 1 μg/mL of cortisol. These cells were cultured in an atmosphere of 5% CO_2 at 37°C.

In vitro growth inhibition assay

The growth inhibitory effects of BIBF 1120 on the HepG2, HLF, HLE, and Huh7 cell lines were examined using an MTT assay as previously described (17, 18). The optical density was measured at 570 nm. Three independent experiments were conducted.

Western blot analysis

The antibodies used for the Western blot analysis were anti-KDR (IBL), anti–phospho (p)-VEGFR2 (Tyr1175), anti-VEGFR1, anti-p44/42 MAPK (mitogen-activated protein kinase), anti–p-p44/42 MAPK, anti–c-Kit, anti-PDGFRβ, anti-FGFR1, 2, and 3, horseradish peroxidase–conjugated secondary antibody (Cell Signaling Technology), and anti–β-actin (Santa Cruz Biotechnology). The methods have been previously described (18). Two independent immunoblotting experiments were conducted.

Tube formation assay

HUVECs were cultured without VEGF-A for 24 hours. A total of 40 μL of Matrigel (BD Bioscience) and 20 μL of PBS were mixed and incubated in 96-well plates. After the gel had solidified, a 100-μL volume of HUVECs (2×10^4 cells/well) was seeded onto the plates with 20 ng/mL of VEGF-A and the indicated concentration of BIBF 1120. The 96-well plates were then incubated for 4 hours. Capillary morphogenesis was evaluated under a microscope (Olympus). This assay was carried out in 3 independent experiments.

Real-time reverse transcriptase PCR

The method has been previously described (17). The primers used for real-time reverse transcriptase PCR (RT-PCR) are shown in Supplementary Table 1. *GAPD* was used to normalize the expression levels in the subsequent quantitative analyses.

Flow cytometric analysis for HUVECs

HUVECs were seeded on 6-well plates without VEGF-A for 24 hours. After exposure to BIBF 1120, AG1478, or 5FU for 3 hours, the cells were stimulated with 20 ng/mL of VEGF-A for 30 minutes. The flow cytometric procedure was carried out according to the manufacturer's protocols,

Published OnlineFirst December 3, 2010; DOI:10.1158/1078-0432.CCR-09-2755

using the Fixation/Permeabilization Kit (BD Biosciences); the data were obtained using a FACSCalibur flow cytometer (BD Biosciences). Anti-phosphotyrosine (pTyr) antibody (P-Tyr-100; Cell Signaling) was used to detect the phosphorylation levels.

Flow cytometric analysis for PBLs in the *in vivo* model

In the *in vivo* model, about 0.5 to 1 mL of peripheral blood was obtained from treated mice and 20 ng/ mL of VEGF was added to the whole blood samples for 20 minutes. The red cells were then lysed using a lysis buffer (155 mmol/L NH_4Cl, 10 mmol/L $NaHCO_3$, and 1 mmol/L EDTA2Na, pH 7.3) for 10 minutes, and leukocytes were fixed and permeabilized using a Fixation/Permeabilization Kit for analysis. The following antibodies were used: anti-mouse CD45-PerCP, anti-mouse Flk-1-PE (BD Biosciences), anti-pTyr (P-Tyr-100; Cell Signaling), and Alexa Fluor Mouse IgG1 Isotype Control (BD Parmingen). The analysis was carried out using the WinMDI software (20).

HCC xenograft model

Nude mice (BALB/c nu/nu; 6-wk-old females; CLEA Japan Inc.) were used for the *in vivo* studies and were cared for in accordance with the recommendations for the handling of laboratory animals for biomedical research, compiled by the Committee on Safety and Ethical Handling Regulations for Laboratory Animal Experiments, Kinki University. The ethical procedures followed and met the requirements of the United Kingdom Coordinating Committee on Cancer Research Guidelines.

Mice were subcutaneously inoculated with a total of 6×10^6 HepG2 cells. Two weeks after inoculation, the mice were randomized according to tumor size into 3 groups to equalize the mean pretreatment tumor size among the 3 groups ($n = 6$ in each group). The mice were then treated with BIBF 1120 (50 mg/kg/d, p.o.), BIBF 1120 (100 mg/kg/d, p.o.), or the vehicle control (saline, p.o.) for 14 days (Fig. 3A–C). On day 14, the mice were euthanized, blood samples were collected by cardiac puncture, and tumor specimens were collected for immunohistochemistry. The tumor volume was calculated as the length $\times$ width$^2 \times 0.5$ and was assessed every 2 to 3 days.

Immunohistochemical analysis

A mouse anti-CD31 monoclonal antibody (1:100; BD Biosciences) was used to detect the endothelial cells. The paraffin-embedded samples were cut into 4-μm sections, deparaffinized, and placed in a preheated antigen retrieval solution (Dako) in a steamer for 10 minutes. All the samples were then blocked in 3% H_2O_2 in methanol for 15 minutes and rinsed with PBS. The slides were then placed in a Sequenza slide staining system (Thermo Fisher Scientific) and blocked in 1% normal goat serum for 20 minutes. The slides were incubated overnight at 4°C with the CD31 antibody. A standard avidin–biotin peroxidase complex assay was then carried out using the ABC Elite Kit (Vector Laboratories). The slides were developed with 3,3′-diaminobenzidine (DAB; Zymed Laboratories) and counterstained with 10% hematoxylin. Microvessel density (MVD) was quantified by measuring the number of CD31-positive endothelial cells in the tumors. Ten random fields per tumor sample at 200× magnification were captured and saved for computer-assisted image analysis using the ImageJ software package (21). An algorithm for color deconvolution was used to segregate the brown DAB-positive CD31 endothelial cells and the blue tumor cells. Thresholds were adjusted to remove background and nonspecific signals. MVD was reported as the average ratio of CD31-positive cells to tumor cells.

Statistical analysis

The statistical analyses were carried out using Microsoft Excel (Microsoft) to calculate the SD and to test for statistically significant differences between the samples using a Student's t test. A value of $P < 0.05$ was considered statistically significant.

Results

BIBF 1120 potently inhibits VEGFR2 signaling in HUVECs

We evaluated the inhibitory effect of BIBF 1120 at various concentrations (0.0001–10 μmol/L) on VEGFR2 signaling, using HUVECs stimulated with 20 ng/mL of VEGF. BIBF 1120 at a concentration of 0.01 μmol/L completely inhibited the phosphorylation of VEGFR2 and MAPK in HUVECs (Fig. 1A). BIBF 1120 at a concentration of 0.01 μmol/L partially inhibited tube formation in HUVECs stimulated with VEGF, whereas BIBF 1120 at a concentration of 1 μmol/L completely inhibited tube formation (Fig. 1B). These data indicate that BIBF 1120 potently inhibits VEGFR2 signaling in endothelial cells.

Flow cytometry detects BIBF 1120–induced inhibition of pTyr levels

To detect the BIBF 1120–induced inhibition of pTyr levels by flow cytometry, the VEGF-induced pTyr levels of proteins in HUVECs were evaluated after exposure to BIBF 1120, the EGFR TKI AG1478 as a TKI control, or 5FU as a cytotoxic drug control. The controls agents were used to show that another target of TKI did not induce (AG1478) or to exclude the possibility that nonspecific effects such as cytotoxic cellular responses were not induced (5FU). Flow cytometry revealed that the VEGF-induced pTyr levels in HUVECs were significantly inhibited by BIBF 1120 at concentration of 1 and 5 μmol/L but not by AG1478 or by 5FU (Fig. 1C and D). This flow cytometric method is considered a feasible means of detecting the inhibition of VEGF-induced pTyr levels induced by VEGFR2 TKIs.

Growth inhibitory effects and expression status of targeted receptors in HCC cell lines *in vitro*

To evaluate the expression status of the putative targeted receptors of BIBF 1120 in the 4 HCC cell lines and HUVECs as a control, we examined the protein expression levels of VEGFR1, VEGFR2, FGFR1, FGFR2, FGFR3, PDGFRβ, and

Published OnlineFirst December 3, 2010; DOI:10.1158/1078-0432.CCR-09-2755

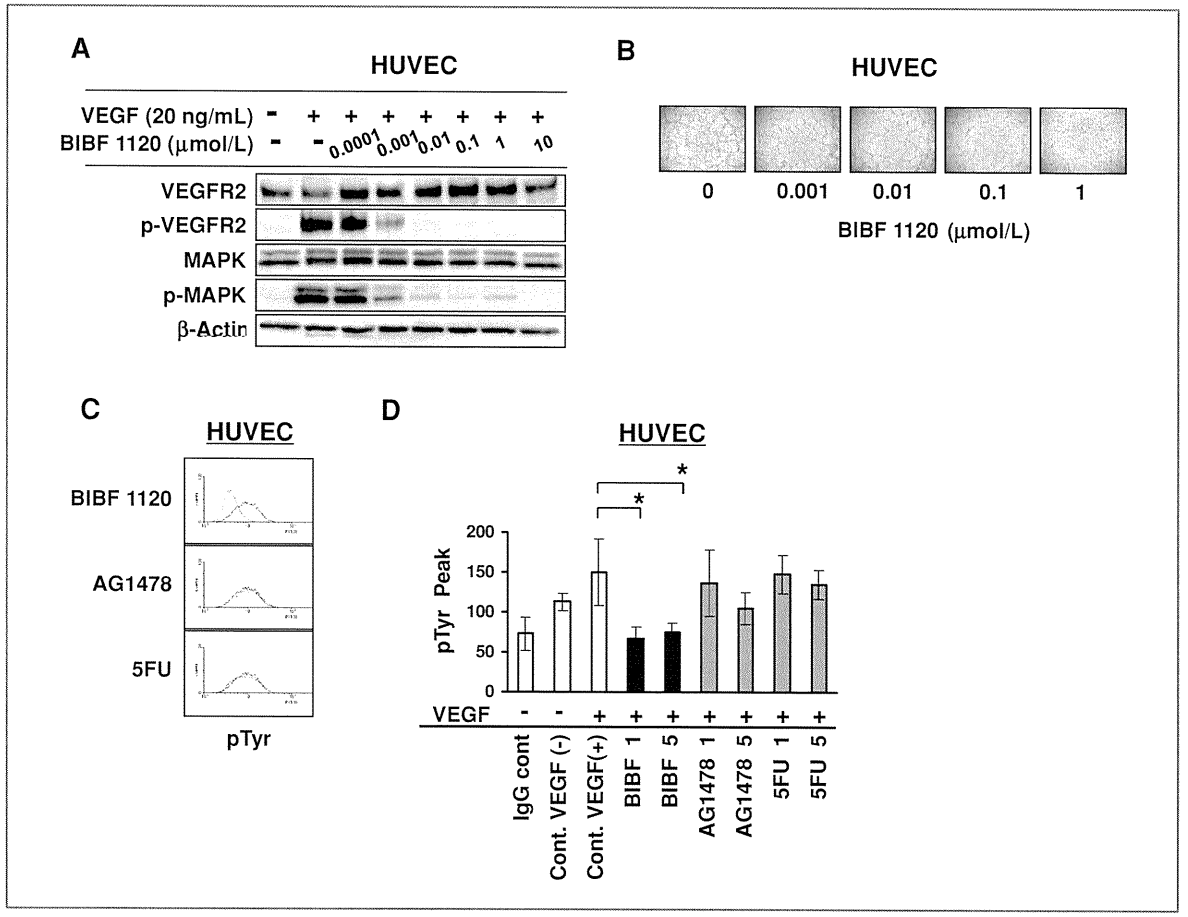

Figure 1. Inhibition of VEGFR2 signaling by BIBF 1120 and detection of the inhibition of pTyr by flow cytometry in HUVECs. A, the inhibition of VEGFR2 and MAPK phosphorylation by BIBF 1120 was determined using a Western blot analysis. HUVECs cultured in a medium containing 2% FBS were exposed to BIBF 1120 (0.0001–10 μmol/L) for 3 hours, stimulated with 20 ng/mL of VEGF for 15 minutes, and lysed for analysis. B, effect of BIBF 1120 on the inhibition of tube formation. HUVECs were seeded with 20 ng/mL of VEGF-A and exposed to BIBF 1120 (0.001–1 μmol/L) on Matrigel-layered 96-well plates for 4 hours. Capillary morphogenesis was evaluated under a microscope. This assay was conducted in 3 independent experiments. C and D, HUVECs were seeded on 6-well plates without VEGF-A for 24 hours. After exposure to BIBF 1120, AG1478, or 5FU for 3 hours, the cells were stimulated with 20 ng/mL of VEGF-A for 30 minutes. The inhibition of pTyr level was detected by flow cytometry with an anti-pTyr antibody. Note that only BIBF 1120 significantly inhibited the VEGF-induced phosphorylation levels of tyrosine. This assay was conducted in 3 independent experiments; bars, SD. *, $P < 0.05$.

c-Kit (the kinase activities of which are reportedly inhibited by BIBF 1120 (15) and p-VEGFR2, MAPK, and p-MAPK by Western blotting. The protein expression of these receptors were not highly upregulated in any of the HCC cell lines, except for PDGFRβ in HLE and HLF cells (Fig. 2A). A comparable expression level of MAPK was observed among the cell lines, and an increase in p-MAPK expression was observed in HLE cells. The mRNA expression levels of the target receptors *VEGFR1*, *VEGFR2*, *VEGFR3*, *PDGFRA*, *PDGFRB*, *FGFR1*, *FGFR2*, *FGFR3*, and *FGFR4* were determined using real-time RT-PCR in the HUVEC line and the HCC cell line. Higher receptor expression levels were observed for *VEGFR2* in HUVECs, *PDGFRB* in HLE and HLF, *FGFR1* in HUVECs and HLE, *FGFR3* in HepG2, and *FGFR4* in Huh7 (Fig. 2B). The expression levels were consistent with the Western blotting results.

We next evaluated the direct growth inhibitory activity of BIBF 1120 in 4 HCC cell lines *in vitro*. The IC_{50} value of BIBF 1120 for the HLE, HLF, HepG2, and Huh7 cell lines were 2.7 ± 1.7, 2.7 ± 0.5, 5.3 ± 0.6, and 4.3 ± 0.9 μmol/L, respectively (Fig. 2C). These results indicate that the direct growth inhibitory activity of BIBF 1120 against HCC cells was relatively mild (IC_{50}: 2–5 μmol/L).

BIBF 1120 potently inhibits tumor growth and angiogenesis of HCC xenografts *in vivo*

Next, we examined the antitumor and antiangiogenic effects of BIBF 1120 *in vivo*. Mice inoculated with HepG2